Stone Columns Field Test: Monitoring Data and Numerical Analyses

Marcio Almeida[1], Bruno Lima[2], Mario Riccio[3], Holger Jud[4], Maria Cascão[5], Felipe Roza[6]

[1]*Geotechnical Laboratory, Federal University of Rio de Janeiro, Rio de Janeiro, Brazil.*
[2]*Fluminense Federal University, Niterói, and FUGRO In Situ Geotecnia, Rio de Janeiro, Brazil.*
[3]*Geotechnical Laboratory, Federal University of Rio de Janeiro, Rio de Janeiro, Brazil.*
[4]*SmoltczykPartner, Germany*
[5]*Polytechnic School of Engineering, Federal University of Rio de Janeiro, Rio de Janeiro, Brazil.*
[6]*VALE Company, Rio de Janeiro, Rio de Janeiro, Brazil.*
[1]*E-mail*: almeida@coc.ufrj.br
[2]*E-mail*: brunotlima@yahoo.com.br
[3]*E-mail*: mvrf1000@gmail.com
[4]*E-mail*: Jud@smoltczykpartner.de
[5]*E-mail*: mariacascao@poli.ufrj.br
[6]*E-mail*: felipe.roza@vale.com

ABSTRACT: This paper presents a case study of a field test performed on a set of 16 stone columns (4 × 4 square mesh, 1.85 m spacing, 1.0 m diameter, and 11.25 m length) loaded with iron rails applied during approximately one month. Extensive instrumentation comprising 28 instruments was used for monitoring the field test area. The objective of this study was to verify the performance of foundation improvements with stone columns for a future ore stockyard. The field test was also useful to calibrate a numerical model for predicting the behaviour of the permanent stockyard. Two- and three-dimensional finite element analyses were carried out and the results of field measurements and numerical calculations were compared. In general the numerical calculations of vertical and horizontal displacements reproduced the field measurements with satisfactory accuracy up to limit state conditions. Calculations of excess pore pressure and total horizontal stresses had less satisfactory agreement, and some reasons are provided for this. The yield of stone columns provided by 3D analysis appears to be more realistic than that provided by 2D analysis.

1. INTRODUCTION

Stone columns are one of the most versatile and frequently used ground improvement techniques worldwide, due their capacity to reduce and accelerate settlements, increase soil bearing capacity, and improve global stability.

Stone columns were probably first used by French military engineers in 1830 to provide heavy foundation support for cast iron resting on soft soil deposits located in an estuary (Hu, 1995). The FHWA (1983) published a report with the basic principles, column types, equipment, and other details about construction and quality. The vibro replacement method of constructing stone columns is described by Hu (1995), Raju et al. (2004), and Yee and Raju (2007).

Among the classical methods of analyzing stone columns, the calculation methods presented by Greenwood (1970), Hughes and Withers (1974), Thorburn (1975), Aboshi et al. (1979), Balaam and Booker (1981, 1985), and Priebe (1995) can be highlighted. More recently Pulko and Majes (2005), Castro (2008), and Castro and Sagaseta (2009) have presented calculation methods that consider the yielding of stone columns.

Aiming at a better understanding of the behaviour of its stockyard soft soil foundation, the ThyssenKrupp Company (TKCSA), located in Itaguaí District, Rio de Janeiro, Brazil, decided to perform a field study. The ground improvement technique prescribed was stone columns, with vibro replacement, and the study combined field studies and 2D and 3D finite element analyses.

To achieve this, a full-scale field test was carried out inside the stockyard area on the clay foundation, which was improved with stone columns. This field test aimed to reach stress levels of similar order of magnitude as those used in the actual stockyard.

2. GEOTECHNICAL PROFILE AND SOIL PROPERTIES

The geotechnical soil profile of the area is shown in Figure 1. An upper soft soil layer, 6.5 to 7.5 m thick, characterizes this profile. A sand layer (1.0 to 3.0 m thick) is found underneath followed by another soft clay layer whose thickness varies from 3.0 to 5.0 m. The remaining soil profile consists mainly of sand layers, quite often without continuity.

A similar stratigraphy has been observed at other coastal areas in Brasil, in Santos (Massad, 1994) and at Barra da Tijuca, Rio de Janeiro (Almeida and Marques, 2011).

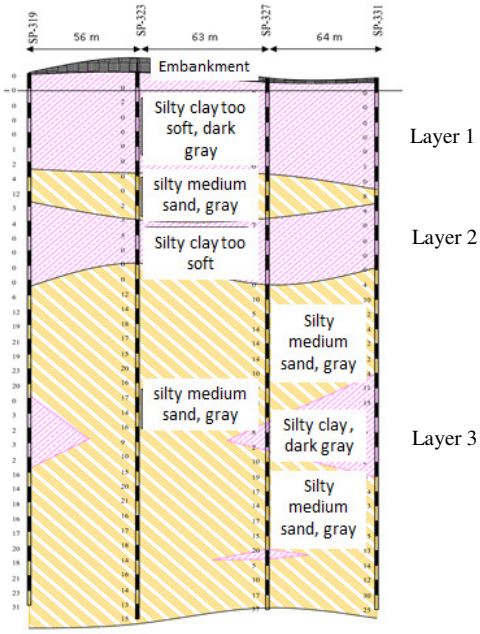

Figure 1 Typical geotechnical profile of the field test area (Lima, 2012)

The geotechnical site investigation campaign involved 14 standard penetration test boreholes (SPT), 20 cone penetration test (CPTu) verticals with pore pressure dissipation, three vane test verticals, six dilatometer test (DMT) verticals, and 16 undisturbed samples extracted with stationary Shelby piston tubes. This

campaign was carried out in a larger area covering the test area (In Situ Geotecnia, 2006). Although performed (in mid-2000) within a design-performance scope, the geotechnical investigation provided the necessary soil parameters to be used in the numerical analyses.

SPT boreholes reached a maximum depth equal to 51.6 m and piezocone tests achieved depths of up to 36.2 m. Vane tests were performed in the first and second clay layers with depths varying from 1.0 to 12.0 m. CPTu dissipation tests were performed to determine the horizontal consolidation coefficient (c_h) at depths ranging from 1.50 to 18.50 m.

A summary of the index parameters of the three soft soil layers is shown in Table 1. Campos (2006) found an organic matter value equal to 3.6% for a nearby area, justifying the low value of G_s obtained.

Table 1 Soil parameters of soft soil in the three layers

Parameter	Value
I_p	30 to 120 %
w_n	32.6 to 142.9 %
Percentage of clay (grain size analysis)	44 to 76%
G_s	2.50 to 2.62
Organic matter content (Campos, 2006)	3.6%

* Ip = plasticity index; wn = natural water content; Gs = specific weight of solid particles

The clay strength was obtained from vane tests, UU and CIU triaxial tests, and piezocone tests (correlated with vane tests). The results of the vane tests are presented in Figure 2. The high values of S_u presented in Figure 2 are associated with sand lenses. The increase in S_u with depth, a well-known behaviour, is observed in Figure 2. The corrected S_u design strength profile combining CPTu and vane tests is shown in Figure 3. Values of N_{kt} were calculated for each depth at which vane tests were performed, and the average value of N_{kt} obtained was equal to 10.7. The Bjerrum (1973) correction factor used in Figure 3 was μ= 0.65, corresponding to I_P = 97%. Although less relevant for stone column projects, the corrected strength profile is presented here for completeness.

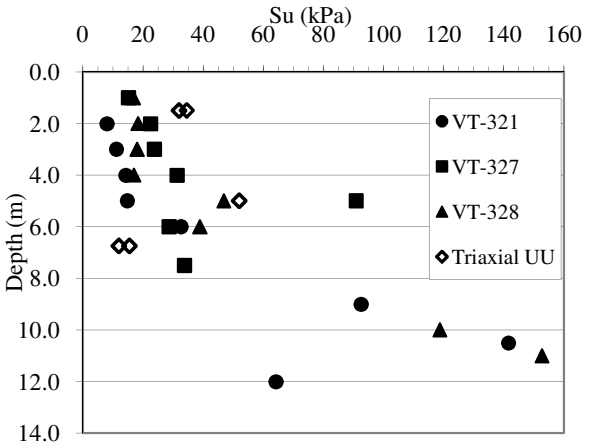

Figure 2 Undrained strength S_u obtained by vane and UU triaxial tests (Lima, 2012)

The quality of TKCSA samples was assessed using the criteria proposed in Coutinho (2007) adapted from Lunne et al. (1997) for Brazilian clays and in general, the tested samples showed good quality. The data presented in Table 2 summarize the parameters obtained from samples taken in the three clay layers.

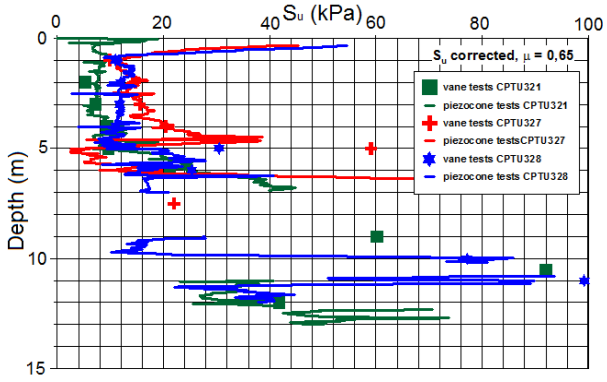

Figure 3 Corrected undrained strength S_u profiles: vane and piezocone tests (Lima, 2012)

Table 2 Soil parameter values for layers 1 to 3 (Lima, 2012)

Parameters	Layer 1	Layer 2*	Layer 3*
CR	0.387	0.367	0.345
RR	0.065	0.040	0.036
C_c	1.59	1.07	1.00
C_s	0.27	0.13	0.12
e_0	3.11	1.91	1.90
c_v [m²/sec]×10^{-8}	2.50	4.45	4.45
OCR	2.7	1.2	1.2
γ [kN/m³]	13.3	15.5	15.5
ϕ' [degrees]	25.0	25.0	25.0

* Data from Marques et al. (2008). CR = $C_c/(1+e_0)$; RR = $C_s/(1+e_0)$; C_c = compression index; C_s = swelling index; e_0 = initial void ratio; c_v = vertical consolidation coefficient; OCR = overconsolidation ratio, γ = soil bulk weight; ϕ' = friction angle obtained from CIU tests

The correlation between C_c and w_n obtained for the three clay layers was found to be $C_c = 0.0125w_n$, quite close to $C_c = 0.013w_n$ obtained by Almeida et al. (2008).

Geotechnical parameters reported in Table 2 were compared with other deposits within TKCSA (Marques et al., 2008) and nearby (Campos, 2006; Aragão, 1975) and overall consistency was found.

The coefficient of vertical permeability (k_v) was calculated based on values of c_v obtained from oedometer tests. Figure 4 shows the variation in k_v with the voids ratio for layer 1. The slope of the e *versus* log k_v data is the parameter C_k, which is equal to 1.27 for layer 1 and 0.65 for layers 2 and 3. These values are smaller than that given by the correlation $C_k = 0.5 \cdot e_0$ (Tavenas et al., 1983).

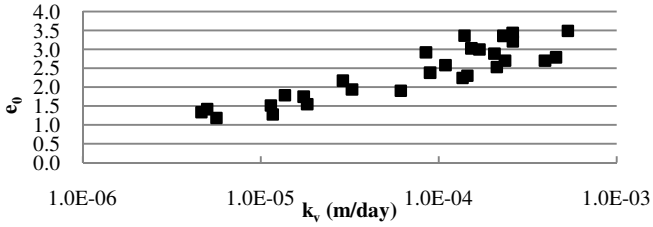

Figure 4 Relation between the vertical coefficient of permeability k_v and the void ratio e_o (Lima, 2012).

3. FIELD TEST AND INSTRUMENTATION

The test field was located in an area inside the future Stockyard area, and the main purposes were to verify the performance of the installed stone columns. Thus, the tested columns had the same design and characteristics of the others columns installed on the Stockyard area.

The field test is shown in Figures 5, 6 and 7, where the surcharge composed of rails laid over a concrete slab may be seen. The field test was performed on 16 stone columns within the ore yard, in a mesh of 4 × 4 columns, with plan dimensions of 6.5 m × 6.5 m. The columns have a diameter of around 1.0 m and are spaced 1.85 m apart, as shown in Figure 6. As the test field was part of the quality measures for the constructed soil improvement the test was located within an area where the soil improvement for the stockyard was initially started. All dimensions as grid and column length therefore derived from the stockyard design, which was based on the investigative reports and the clients load assumption for the stockyard.

With the objective of creating a span between the rails and the ground surface and preventing contact of the rails with the soil, four concrete beams (6.50 m × 0.40 m × 0.40 m) were inserted above the steel plate (Figures 5 and 6). The surcharge was applied in steps, and after 27 days the maximum load of 180 kPa was achieved. Unloading, also in steps, followed loading.

The field instrumentation, composed of 28 instruments (see Figures 6 and 7), consisted of:

- Eleven settlement plates (S), installed in one vertical, at 0.50 m depth, below three concrete beams (settlement plate S6 was damaged);
- Two inclinometers (I), with lengths of 23.0 m and readings every 0.50 m, positioned on the west side of the test area 0.75 and 6.05 m from the concrete slab edge;
- Nine vibrating wire piezometers (P). Four piezometers were installed together with a total stress cell (EP). The installation depths were 4.0, 4.5, 6.0 (two sensors), 7.0, 7.5, 8.3 (damaged sensor), 11.7, and 12.0 m;
- Two magnetic extensometers (EX). Sensors were at depths of 6.0, 11.0, 14.0, 23.5, and 27.0 m. Three boreholes were used for this.
- Four total stress cells (EP) inserted vertically, with the objective of measuring the variation in horizontal effective stress. These instruments were installed at depths of 4.5, 6.0, 7.5, and 8.3 m (damaged sensor).

Figure 5 Field test with rails surcharge (TKCSA, 2007)

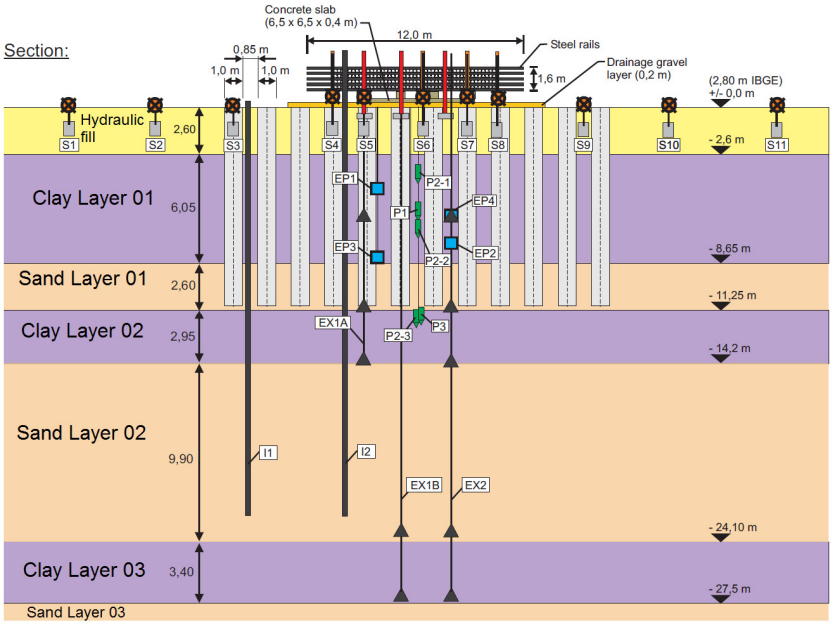

Figure 6 Soil profile, column spacing and diameter, and test area instrumentation (TKCSA, 2007)

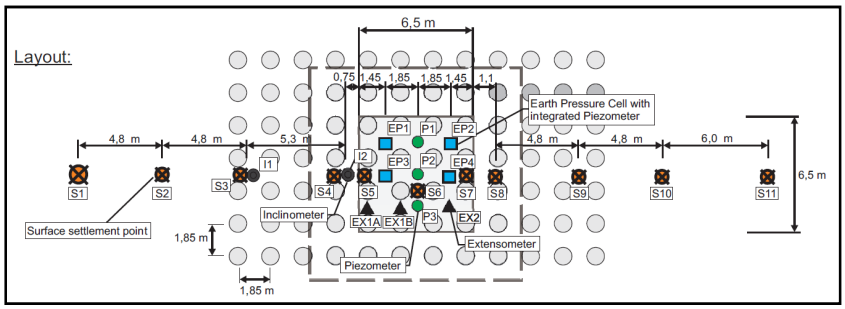

Figure 7 Layout of the test area (TKCSA, 2007)

Table 3 presents the chronological sequence of the events related to the test area, including the time required to build the working platform and column installation. The working platform was constructed by means of a hydraulic fill to allow the works to be carried out over a superficial soft soil layer. Stages named "Consolidation" in Table 3 refer to periods without load increase. Figure 8 shows the load schedule (vertical applied stress) and its magnitude in the test area.

Table 3 Field test loading schedule (TKCSA, 2007)

Stage	Description	Loading [kPa]	Duration [days]
0	Initial conditions	–	–
1	Working platform construction (dredged sand fill)	–	182
2	Consolidation (fill layer)	–	90
3	Column installation	–	5
4	Consolidation (column installation)	–	60
5	Concrete slab installation	–	18
6	Loading 01 (beginning 19 June 2008 – day 0 in this analysis)	102.25	16
7	Consolidation 01 (beginning 5 July 2008)	102.25	2
8	Loading 02 (beginning 7 July 2008)	112.23	1
9	Consolidation 02 (beginning 8 July 2008)	112.23	1
10	Loading 03 (beginning 9 July 2008)	150	3
11	Consolidation 03 (beginning 12 July 2008)	150	1
12	Loading 04 (beginning 13 July 2008)	183.6	3
13	Consolidation 04 (beginning 16 July 2008)	183.6	1
14	Unloading (beginning 17 July 2008)	126.0	4
15	Consolidation post-unloading (beginning 21 July 2008)	126.0	16

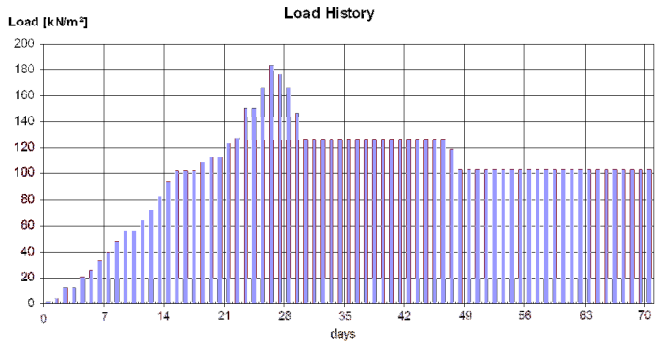

Figure 8 Loading sequence in the test area (TKCSA, 2007)

4. MODELLING AND CONSTITUTIVE LAWS

4.1 Geomechanical model of the field test area

The field test area is presented in Figures 6 and 7. For better visualization only the central stone columns are drawn, but columns were installed in the whole stockyard.

The soil profile consists of a 2.6 m sand fill (working platform/load transfer platform) followed by a 5.65 m thick clay layer, a 2.6 m thick sand layer, and another 2.95 m thick clay layer. This profile was determined through CPTu tests performed (three months before the beginning of field loading) after the installation of stone columns and working platform (TKCSA, 2007).

Stone columns were driven through the working platform, first clay layer, and sand layer to a depth of 8.45 m, with a total length of 11.25 m. After the installation of columns, the test area was cleaned and flattened. A gravel layer of 0.20 m was introduced to work as a drainage layer.

In the test area the ground level was +2.80 m and the water table level was +2.00 m to (TKCSA, 2007).

The construction of the working platform (dredged sand layer) and the period that followed (see Table 3) resulted in consolidation of the clay layers. So, calculations based on Terzaghi theory and on numerical analyses were carried out to update some parameters of the clay layers. These new parameters are presented in Table 4.

Numerical analyses indicated quite small values of excess pore pressure (around 2 kPa) in the clay layers at the beginning of the field test. Data from piezometers installed in clay layer 1 did not indicate any excess pore pressure before loading. Therefore, it was considered that at the beginning of the loading there was no excess pore pressure to be dissipated in the clay layers induced by the construction of the working platform.

Table 4 Updated parameters for clay layers after construction of the working platform (Lima, 2012)

Layer	Parameters					
	K_0	e_0	γ [kN/m³]	OCR	$k_v \times 10^{-5}$ [m/day]	$k_h \times 10^{-5}$ [m/day]
Clay 1	0.60	2.97	13.4	1.08	20.0	40.0
Clay 2	0.60	1.68	16.0	1.08	3.9	7.8
Clay 3	0.60	1.85	15.6	1.08	7.1	14.2

4.2 Constitutive models and material modelling

Clay layers were modelled in the program PLAXIS with the Soft Soil model (Brinkgreve, 2010), a Cam-Clay type model.

Clay layer 1, through which the stone columns were driven, was considered smeared during columns installation; that is, the coefficients of permeability were reduced. The ratio between the diameter of the smear zone and diameter of the stone column was considered equal to 2.0 (Weber, 2008).

Initially, a parametric analysis was carried out so that three parameters with some degree of uncertainty could be assessed: the friction angle of the stone column gravel material ϕ', the earth pressure coefficient after column installation (K^*), and the coefficients of vertical and horizontal permeability of the clay layers following column installation. This study was done due to the lack of data for these parameters (Lima, 2012).

Model evaluation was done through comparison between numerical results and field measurements. The range of values for the friction angle of stone columns is 38° to 45° (FHWA, 1983; Besançon et al., 1984; Mitchell and Huber, 1985; Mestat et al. 2006; Bouassida et al. 2009; Foray et al. ,2009). The best fit provided by the parametric analysis (Roza, 2012) was a column friction angle ϕ' = 40°, K^* = 1.25 (up to a column installation depth of –8.45 m), and ratio of the permeability coefficient before and after installation equal to 5.0. The obtained value of K^* = 1.25 is similar to the magnitude of K^* provided by Pitt et al. (2003), Elshazly et al. (2006), Guetif et al. (2007), Elshazly et al. (2008), and Choobbasti et al. (2011).

These values were used in the numerical analyses presented ahead. Table 5 summarizes the parameters used for the clay layers.

The linear elastic perfect plastic Mohr-Coulomb model was adopted for all granular materials involved in the analyses. Table 6 presents the parameters adopted for the stone column, hydraulic fill working platform and sand layers.

The concrete slab material was assumed to be a linear elastic plate finite element and the parameters adopted are presented in Table 7.

Table 5 Parameters for clay layers - Soft Soil model (Lima, 2012)

Material	Clay layer 1	Clay layer 2	Clay layer 3
γ[kN/m^3]	13.4	16.0	15.6
ϕ'[º]	25.0	25.0	25.0
c'[kPa]	0.0	0.0	0.0
K* or K$_0$[–]	1.25	0.60	0.60
C$_c$ [–]	1.92	1.07	1.00
C$_s$ [–]	0.29	0.13	0.12
C$_a$ [–]	0.04	0.04	0.04
e$_0$[–]	2.97	1.68	1.85
OCR [–]	1.08	1.08	1.08
k$_x$ [m/day]	7.9×10^{-5}	7.8×10^{-5}	14.0×10^{-5}
k$_x$ [m/day]	3.9×10^{-5}	3.9×10^{-5}	7.0×10^{-5}
C$_k$[–]	1.27	0.60	0.60

Table 6 Parameters for granular layers – Mohr-Coulomb model (Lima, 2012)

Material	γ [kN/m³]	K$_0$ [–]	ϕ' [°]	*E'* [kPa]	ν' [–]
Stone column	20.0	0.35	40.0	80.000	0.3
Hydraulic fill	18.0	1.25	30.0	2.000	0.3
Sand 01	18.0	1.25	30.0	30.000	0.3
Sand 02	18.0	0.50	30.0	30.000	0.3
Sand 03	18.0	0.50	30.0	250.000	0.3

E' = Young's modulus; ν' = Poisson ratio

Table 7 Parameters for the concrete slab – Linear Elastic Model (Lima, 2012).

Material	γ [kN/m³]	E.A [kN/m]	E.I [kNm²/m]	ν [–]
Concrete slab	25.0	1.2×10^7	1.6×10^5	0.2

5. TWO-DIMENSIONAL NUMERICAL ANALYSIS

The finite element (FE) model adopted (based on the profile shown in Figure 6) is presented in Figure 9. As the FE analysis was 2D the columns needed to be transformed in trenches. For that purpose, Method 2 proposed by Tan et al. (2008) was applied, in which the drainage capacity of the axi-symmetric unit cell and the 2D problem are maintained; thus in the 2D problem the stone columns were modelled as 0.40 m wide trenches.

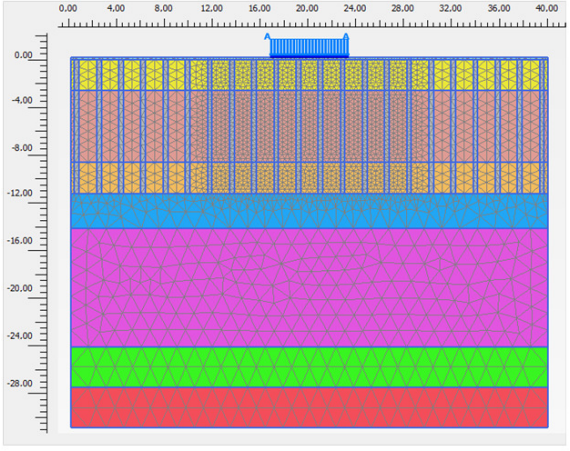

Figure 9 Finite element mesh adopted (Lima, 2012)

The adopted FE mesh (Figure 9) was formed by 5,213 triangular elements with 15 displacement nodes and 12 stress calculation integration points. Boundary conditions considered vertical displacements restrained at the model base, vertical displacement restricted at the sides, and pore pressure flow restrained laterally in the clay layers (Roza, 2012).

The loading and consolidation steps followed the construction steps presented in Table 3 and Figure 8 exactly, including the unloading followed by a consolidation stage. The results of 2D analysis presented in this section are restricted to yield conditions, as complete 2D results will be presented in the next section together with the 3D analysis.

The yield of the stone columns (plastic behaviour) was assessed during the loading and unloading stages and its evolution along the column length is represented by the red points in Figure 10 for selected loading stages.

Column yielding started at the top (Figure 10a) and reached deeper points as loading stages are applied. This behavior is in accordance with the predictions of Castro and Sagaseta (2009) and Six et al. (2012).

In Figure 10b it is possible to notice that the yield state is reached along the whole column length and also that a plastic wedge is formed, which is characteristic of punching failure of superficial foundations. A plastic zone adjacent to this wedge also occurs, as presented by Vesic (1975).

At the end of the unloading stage (Figure 10c) a reversion of columns to the elastic state occurs, but as load transference and consolidation occur, the columns yield again (Figure 10d).

6. THREE-DIMENSIONAL ANALYSIS VERSUS TWO-DIMENSIONAL NUMERICAL ANALYSIS

With the aim of evaluating the results of the 2D analysis and the geometric transformation adopted (Tan et al., 2008) a series of 3D analyses was carried out. Both 2D and 3D results are presented in this section.

Figure 11 shows the 3D numerical model, 0.925 m wide, 20.35 m long, and 18.0 m high, used in the study. In order to reduce the computational effort the analysis was limited to a half space model of column spacing with symmetry passing through the column centres. The FE mesh used 28,930 tetrahedral elements (10 displacement nodes and four Gauss points) for the soil layers and six node-displacement triangular elements for the concrete slab. Boundary conditions were similar to those adopted for the 2D analysis with regard to displacements and pore pressure flow. The material properties and loading conditions were the same as those adopted for the 2D analysis.

The results of the 2D and 3D analyses to be presented for comparison with field measurements are the displacements, pore pressure, and horizontal stresses. The results of yielding points and total displacements (vertical and horizontal) will also be presented.

Limit state conditions appeared to be reached on the 22nd day of loading, when displacements accelerated (observed in the field and in the numerical analyses). Therefore, after this day the numerical analysis may be considered qualitative, because it was not possible for the program to simulate the discontinuous soil mass caused by failure. The use of an elasto-plastic hardening model for the stone columns may overcome this difficulty.

6.1 Displacement results

The results of settlement *versus* time (settlement plates S5, S6, S7, and S8) are compared with the 2D and 3D numerical analyses in Figure 12. It can be observed that after the 22nd day the vertical displacements accelerated at the settlement plates, indicating that the limit state condition was achieved. Good agreement between the numerical analyses (2D and 3D) and measured data is observed during the loading phase up to the 22nd day.

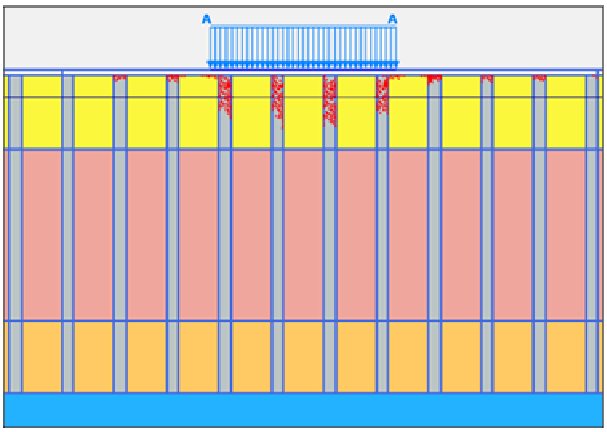

(a) One quarter of the first loading – Stage 6

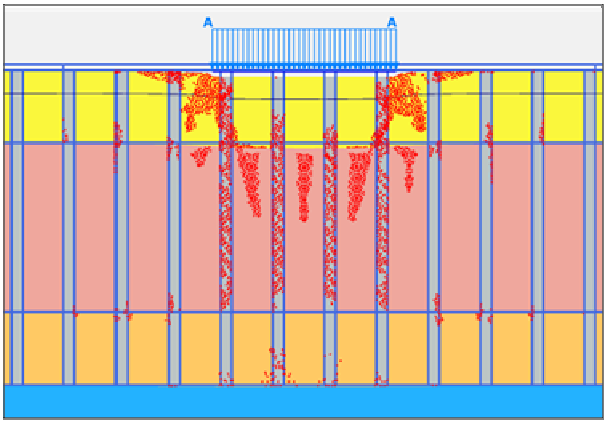

(b) End of the second loading – Stage 8

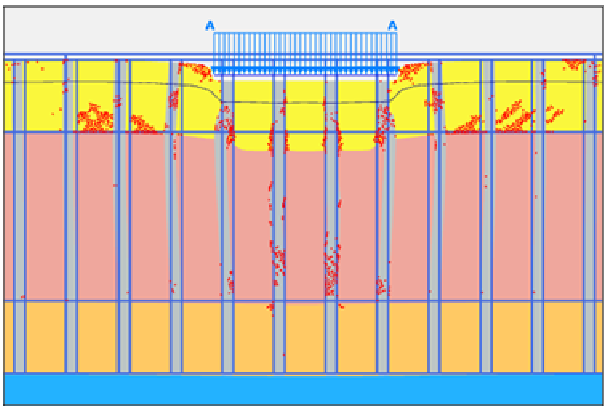

(c) End of the unloading– Stage 14

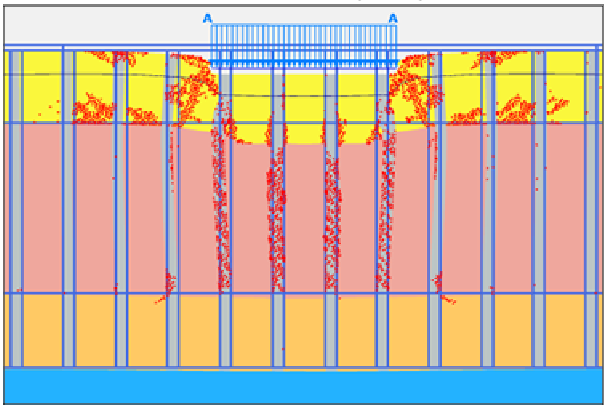

(d) End of consolidation following unloading – Stage 15

Figure 10 Yield points for different analysis stages (Lima, 2012)

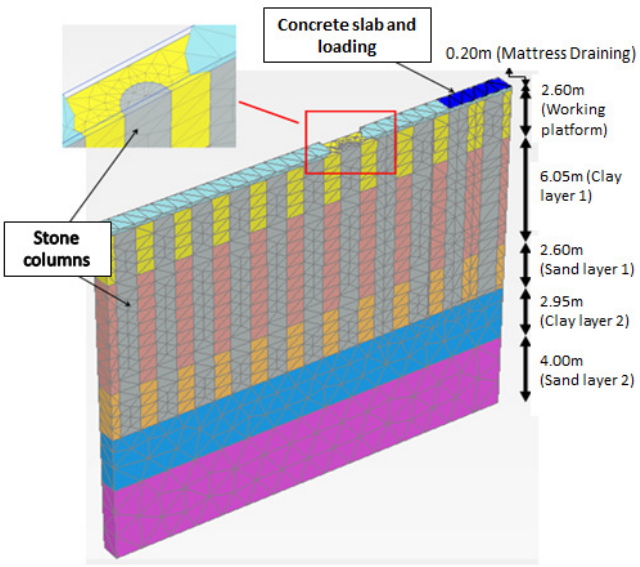

Figure 11 Three-dimensional finite element model and mesh (Lima, 2012)

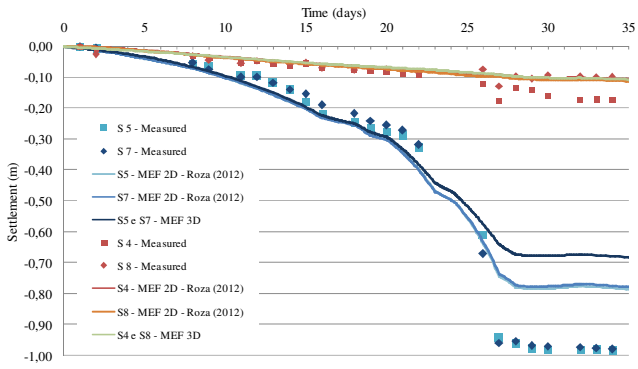

Figure 12 Vertical displacements at plates S5, S6, S7, and S8 – 2D and 3D analyses (Lima, 2012)

Vertical displacements (numerical analysis and instrumentation) along the axis of the test field area are presented in Figure 13. Both numerical analyses, 2D and 3D, were able to reproduce with good accuracy the settlements for all points of measurements, including the soil heave (plates S3 and S9) outside the footprint of the loaded area. Agreement of settlement results between the 2D and 3D analyses suggests that the procedure for geometric transformation was satisfactory.

The uniform pattern of vertical displacements shown in Figure 13 can be compared with the results of total displacements from the 3D analysis shown in Figure 14 at the end of stage 4. It can be observed that the maximum magnitudes of total displacements and vertical displacements are almost the same (0.64 cm for 3D analysis and 0.72 cm for 2D analysis).

The vertical displacements obtained on the magnetic extensometers, at 6,0 and 11,0 m depth, were also compared with the numerical results with good agreement (Lima, 2012).

The numerical results of horizontal displacements and measurements (at inclinometer I2 at depths of 3.5 and 8.0 m) are compared in Figure 15. It is observed that the results of the 3D and 2D analyses are quite close. This result was also obtained on the comparison from the Inclinometer I1 data (Lima, 2012).

Similarly to vertical displacements, horizontal displacements exhibit good agreement between predicted and measured values, and on the 22nd day the displacements at 3.5 m depth accelerate.

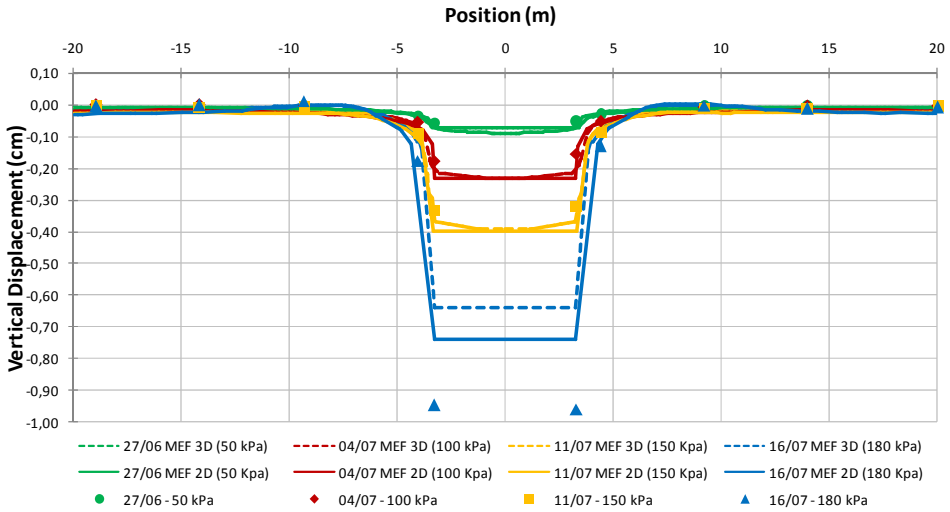

Figure 13 Vertical Displacements along the axis of the field test area – 2D analyses (Roza, 2012)

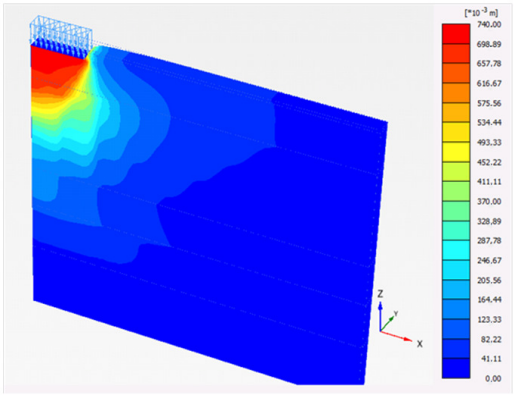

Figure 14 Total displacements along the axis of the field test area in 3D analysis – end of stage 4 before consolidation (Lima, 2012)

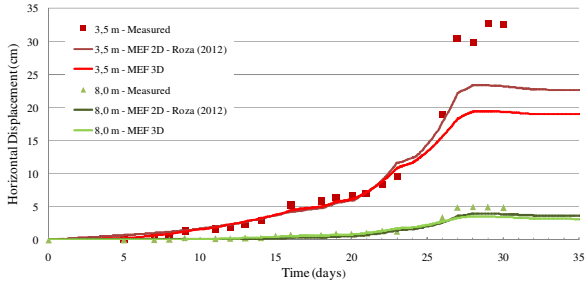

Figure 15 Horizontal displacements – Inclinometer I2 at 3.5 and 8.0 m depth – 2D and 3D analyses (Lima, 2012)

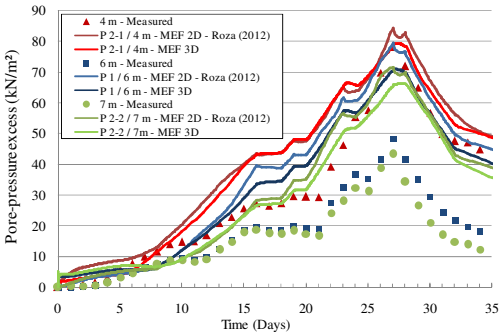

Figure 16 Excess pore pressures – piezometers P1, P2-1, and P2-2 – 2D and 3D analyses (Lima, 2012)

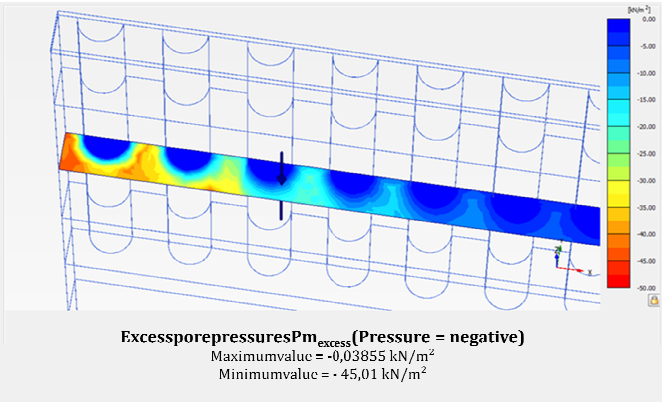

Figure 17 Excess pore pressure at 6.0 m depth – 20th loading day (Lima, 2012)

6.2 Pore pressures and total stresses

The excess pore pressures measured by piezometers located at 4.0, 6.0, and 7.0 m depth are compared in Figure 16 with the corresponding values obtained by numerical analysis. The values obtained by numerical calculations are greater than the measured values, but the curve patterns are quite similar.

The numerical values of excess pore pressure were obtained at the midpoints located exactly between columns. However, in the field this midpoint condition may not exist as the columns and the piezometers may become closer for a number of reasons related to installation issues. Thus, differences could result both from the positioning of piezometers in relation to the stone columns and due to differences in the values of the coefficients of permeability used in the numerical analyses compared to actual field values. Roza (2012) carried out an analysis considering the points adjacent to and in the mid-space between the columns and showed that the measured values lay between these two.

Figure 17 shows the values of excess pore pressure obtained from the 3D analysis at 6.0 m depth on the 20th day. As expected, the obtained values of excess pore pressure are higher in the central positions of the loading application area (left hand columns, Figure 17), and decrease towards the points far from the central loading area. It can be seen that the gradient of excess pore pressure is very pronounced in this situation, with differences of up to 50 kPa (in the region surrounding the stone columns). Therefore, a small difference in the position of the piezometer may cause significant differences in the values of the measured pore pressure.

Total stress cells were installed in the vertical position in the first clay layer to provide values for the increase in total horizontal stress ($\Delta\sigma_h$) during loading. Figure 18 compares measurements of numerical values of $\Delta\sigma_h$ at 4.5, 6.0, and 7.5 m depth. It can be seen in Figure 18 that the numerical analyses reproduced the measured values fairly well, in particular the trend of increasing and decreasing values with time. From the 11th day 'onwards, particularly at 7.5 m depth, the results of 2D and 3D predictions were fairly close to the field data. The differences can be related to the installation procedure resulting in a cell's position not exactly vertically in relation to the horizontal.

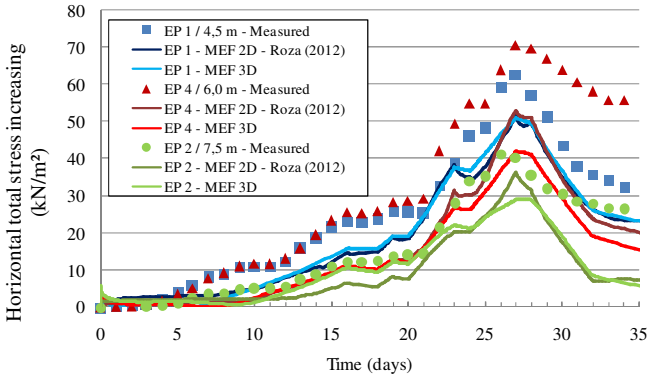

Figure 18 Increase in total horizontal stresses – 2D and 3D analyses Lima (2012).

6.3 Yield for 3D analysis

Yield points determined by 3D analysis are shown in Figure 18 at stages 8 and 14 (see Table 3). Similarly to the 2D analysis at stage 8 (Figure 19a), the stone columns yield along their entire length under the loaded area and a failure wedge can also be observed. Similar behaviour was found in numerical studies performed by Castro and Sagaseta (2009) and Six et al. (2012).

At the end of stage 14 (Figure 19b), it can be seen that there are more yield points than those found in the 2D analysis shown in Figure 10d. This difference is probably due to the fact that arching effects occurring in 3D and 2D analysis are different. Therefore, the proposed method of geometric transformation (3D to 2D) did not correctly reproduce the plastic state in the unloading stage. In previous stages before unloading, the plastic points are very similar in 2D and 3D analyses (Lima, 2012).

7. CONCLUSIONS

This paper described a field test study related to soft ground improved by stone columns loaded up to 180 kPa, which included 2D and 3D finite element analyses. The effects of the working platform and column installation caused variation in the soil properties of the layers and could not be neglected.

In general, vertical and horizontal displacements obtained by numerical predictions showed good agreement with field measurements up to the 22nd day of loading, when the limit state condition was observed, close to failure, which was not adequately modelled in the numerical analyses. Differences between numerical predictions and measurements increased after the 22nd day.

The magnitudes of excess pore pressure predicted by the numerical analyses were generally greater than the measured ones. This difference could be due to inadequacy in modelling the consolidation or due to uncertainties in the exact *in situ* position of the piezometers.

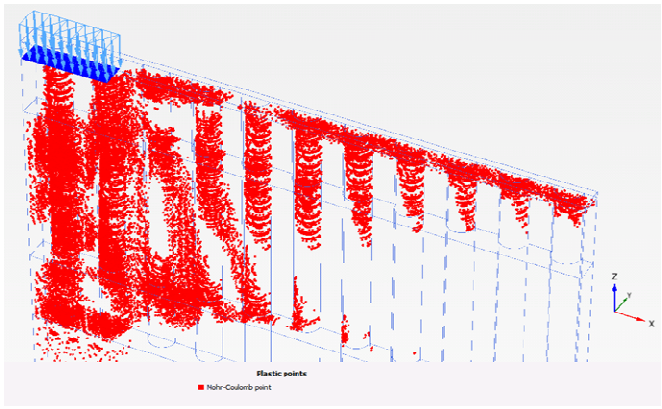

(a) End of the second loading – Stage 8

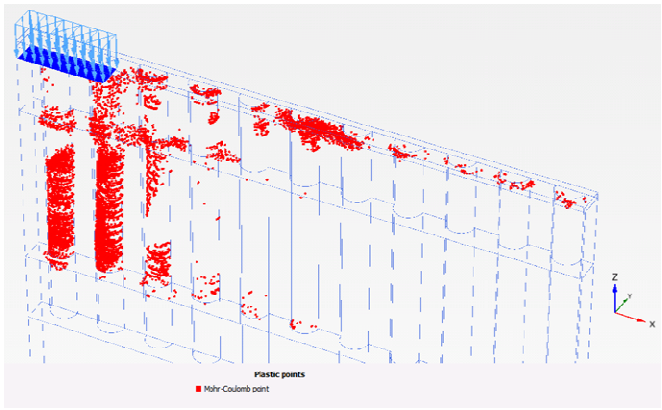

(b) End of the unloading – Stage 14

Figure 19 Yield points of the stone columns – 3D analysis (Lima, 2012).

Values of horizontal stress measured in the field lie in the range of values provided by the numerical calculations. Differences can be related to the position of total stress cells, which could not be installed exactly perpendicular to the test field axis.

It was observed in the numerical analyses that yielding in the columns started at the top and reached greater depths as loading was applied. The plastic points occurred along the whole column depth at the end of the loading stage. In general, the plastic points were similar in the 2D and 3D procedures.

The results of the 2D analysis, based on geometric transformation, were in general similar to those of the 3D analysis, a finding also obtained by Tan et al. (2008).

The present studies showed that field tests could be a powerful tool in large projects when the results are combined with finite element calculations.

The behaviour of the field test could be reproduced quite well which is promising considering that there is not much experience with stone columns in very soft soils.

8. ACKNOWLEDGEMENTS

The studies presented in this paper were performed under an agreement between TKCSA and the Federal University of Rio de Janeiro.

9. REFERENCES

Aboshi, H., Ichimoto, E., Enoki, M., and Harada, K. (1979) The Compozer. A method to improve characteristics of soft clays by inclusion of large diameter sand columns. International Conference on Soil Reinforcement. Reinforced Earth and Other Techniques, Vol. I, Paris, pp. 221–216.

Almeida, M.S.S., Futai, M.M., Lacerda, W.A., and Marques, M.E. S. (2008) Laboratory behavior of Rio de Janeiro Soft Clays. Part 1: Index and compression properties. Soils and Rocks Journal 31, 69–75.

Almeida, M.S.S., Marques, M. E. S. (2011) Construction methods in Brazilian extremely soft soils. In: 14th Panamerican Conference for Soil Mechanics and Geotechnical Engineering, Toronto.

Aragão, C.J.C. (1975) Geotechnical properties of some clay deposits in Rio de Janeiro metropolitan area. Master's dissertation, PUC-RJ, Rio de Janeiro, Brazil [in Portuguese].

Balaam, N.P. and Booker, J.R. (1981). Analysis of rigid rafts supported by granular piles. International Journal for Numerical and Analytical Methods in Geomechanics 5, 379–403.

Balaam, N.P. and Booker, J.R. (1985). Effect of stone column yield on settlement of rigid foundations in stabilized clay. International Journal for Numerical and Analytical Methods in Geomechanics 9, 331–351.

Besançon G., Iorio, J.P., and Soyez B. (1984). Analyse des paramètres de calcul intervenant dans le dimensionnement des colonnesballastées. Proceedings of the International Conference on in situ Soil and Rock Reinforcement, Presses de l´École Nationale des Pontset Chaussées, Paris, pp. 119–126 [in French].

Bjerrum, L. (1973) Problems of soil mechanics and construction on soft clays and structurally instable soils. Proceedings of the 8th International Conference on Soil Mechanics and Foundation Engineering, Moscow, vol. 3, pp. 111–159.

Bouassida, M., Ellouze, S., and Hazzar, L. (2009) Investigating Priebe's method for settlement estimation of foundation resting on soil reinforced by stone columns. Proceedings of the 2nd International Workshop on Soft Soils – Focus on Ground Improvement, Karstunen and Leoni (eds.), Glasgow, CRC Press, pp. 321–325.

Brinkgreve, R.B.J. (2010) Finite Element Code for Soil and Rock Analyses – PLAXIS – 2D User's Manual. Rotterdam, Netherlands, Balkema.

Campos, A.C.S.L. (2006) Compressibility characteristics of a soft clay on the industrial area of Santa Cruz, Rio de Janeiro. Master's dissertation, PUC-RJ, Rio de Janeiro, Brazil [in Portuguese].

Castro, J. (2008) Análisis teórico de la consolidación y deformación al rededor de columnas de grava. D.Sc. Thesis, Cantabria University, Santander, Spain

Castro, J. and Sagaseta, C. (2009) Field instrumentation of an embankment on stone columns. Proceedings of the 17th International Conference on Soil Mechanics and Geotechnical Engineering – ICSMGE 2009. CD-ROM.

Choobbasti, A.J., Zahmatkesh, A., and Noorzad, R. (2011) Performance of stone columns in soft clay: numerical evaluation. Geotechnical and Geological Engineering 29(5), 675–684.

Coutinho, R.Q. (2007), Characterization and engineering properties. Second International Workshop on Characterization and Engineering Properties of Natural Soils Tan, Phoon, Higth, and Leroueil (eds.), Singapore, pp. 2049–2100.

Elshazly, H.A., Hafez, D., and Mosaad M (2006) Back calculating vibro-installation stresses in stone columns reinforced grounds. Journal of Ground Improvement 10(2), 47–53.

Elshazly, H.A., Elkasabgy, M., and Elleboudy, A. (2008) Effect of inter-column spacing on soil stresses due to vibro-installed stone columns: interesting findings. Geotechnical and Geological Engineering 26, 225–236.

FHWA (1983) Design and construction of stone columns, vol 1. Report FHWA/RD-83/027, Barksdale, R.D. and Bachus R.C (eds.), Federal Highway Administration.

Foray, P., Flavigny, E., Nguyen, N.T., Lambert, S., and Briançon, L. (2009) Modélisation numérique 3D de colonnes ballasté es et application. Proceedings of the 17th International Conference on Soil Mechanics and Geotechnical Engineering – ICSMGE 2009. CD–ROM.

Greenwood, D.A. (1970) Mechanical improvement of soils below ground surface. C.R. Conference on Ground Engineering, Institution of Civil Engineers, London, paper II, pp. 11–22.

Guetif. Z., Bouassida, M., and Debats, J.M. (2007) Improved soft clay characteristics due to stone column installation. Computers and Geotechnics 34(2), 104–111, March.

Hu, W. (1995). Physical modelling of group behaviour of stone column foundations. D.Sc. Thesis, Glasgow University, Scotland, p. 312.

Hughes, J.O. and Withers, N.J. (1974) Reinforcing of soft cohesive soils with stone columns. Ground Engineering pp. 42–49.

In Situ Geotecnia (2006) CSA Soil Investigation. Data Book, vol. 04. Technical Report, Brasil, p. 698.

Lima, B.T. (2012) Study on the use of stone columns in very soft soil clays. D.Sc. thesis, COPPE/UFRJ, Rio de Janeiro, Brazil, p. 321.

Lunne, T., Berre, T., and Strandvik, S. (1997) Sample disturbance effects in soft low plastic Norwegian clay. Recent developments in soil and pavement mechanics. COPPE/UFRJ, Rio de Janeiro, pp. 81–102.

Marques, M.E.S., Lima, B.T., Oliveira, J.R.M., Antoniutti Neto, L., and Almeida, M.S.S. (2008) Geotechnical characterization of a compressible soil of Itaguaí, Rio de Janeiro. IV Luso Brazilian Geotechnical Congress, Coimbra. CD-ROM [in Portuguese].

Massad, F. (1994). "Propriedades dos Sedimentos Marinhos". Solos do Litoral de São Paulo, ABMS: 99-128.

Mestat, P., Magnan, J.P., and Ddhouib, A. (2006). Results of the settlement prediction exercise of an embankment founded on soil improved by stone columns. Numerical Methods in Geotechnical Engineering — NUMGE 06, Schweiger (ed.), Graz, Austria, Taylor & Francis Group, Londres, pp. 471–476.

Mitchell, J.K. and Huber, T.R. (1985) Performance of a stone column foundation. Journal of Geotechnical Engineering 3(2), 205–223.

Pitt, J., White, D., Gaul, A., and Hoevelkamp, K. (2003). Highway applications for rammed aggregate piers. Final Report, Iowa DOT Project TR-443.

Priebe, H.J. (1995) The design of vibro replacement. Ground Engineering 28(10).

Pulko, B., and Majes, B. (2005) Simple and accurate prediction of settlements of stone column reinforced soil. 16th International Conference on Soil Mechanics and Geotechnical Engineering, Osaka, Japan, vol. 3, pp. 1401–1404.

Raju, V.R., Hari Krishna, R., and Wegner, R. (2004) Ground improvement using vibro replacement in Asia 1994 to 2004 – A 10 years review. 5th International Conference on Ground Improvement Techniques, Kuala Lumpur.

Roza, F.C. (2012) Behavior of works on soft soils with stone columns, Master's dissertation, COPPE/UFRJ, Rio de Janeiro, Brazil, p. 156 [in Portuguese].

Six, V., Mroueh, H., Shahrour, I., and Bouassida, M. (2012) Numerical analysis of elastoplastic behavior of stone column foundation. Geotechnical and Geological Engineering (1 March), pp. 1–13.

Tan, S.A., Tjahyono, S., and Oo, K.K. (2008). Simplified plane-strain modeling of stone-column reinforced ground. Journal of Geotechnical and Geoenvironmental Engineering 134(2), 185–194.

TKCSA (2007). TKCSA design and quality documents for the soil improvements.

Tavenas, F., Jean, P., Leblond, P., and Leroueil, S. (1983). The permeability of natural soft clays, part II, permeability characteristics. Canadian Geotechnical Journal 20, 645–660.

Thorburn, S. (1975). Building structures supported by stabilized ground. Géotechnique 25 81975(1), 83–94.

Vesic, A.S. (1975). Bearing capacity of shallow foundations. In: Foundation Engineering Handbook, H.F. Winterkorn and H. Y. Fang (eds.), Van Nostrand Reinhold, pp. 121–147.

Weber, T.M. (2008) Modellierung der Baugrundverbesserung mit Schottersäulen. Veröffentlichungen des Institutes für Geotechnik, in Germane, ETH Zürich, Band 232.

Yee, Y.W. and Raju, V.R. (2007) Ground improvement using vibro replacement (vibro stone columns) – historical development, advancements and case histories in Malaysia. 16th Southeast Asian Geotechnical Conference, Kuala Lumpur, Malaysia.